Borehole Tensor Strain Measurements in California

MICHAEL T. GLADWIN, ROSS L. GWYTHER, RHODES HART, AND MAX FRANCIS

Department of Physics, University of Queensland, St. Lucia, Australia

M. J. S. JOHNSTON

U.S. Geological Survey, Menlo Park, California

Two continuous borehole plane strain monitoring sites have been operational in California since late 1983, using borehole tensor strain monitors implanted at a depth of 150 m. Shear strain data at subtidal sensitivies were available immediately after installation without contamination by bond curing or thermal recovery signals. At Pinon Flat Observatory, data indicate a constant shear strain accumulation of 0.6 microstrain per annum with the axis of maximum compression oriented $50° \pm 5°$ west of north. This result differs significantly from regional geodetic estimates, the amplitude being dominated by continued viscoelastic response of the hole. Variations of measured strain rate exceeding 100 nstrain/yr would be significant at this instrument site. At San Juan Bautista, measurements of the angle of maximum compression ($10° \pm 3°$ west of north) agree closely with previous geodetic and hydrofracture estimates. After 2 years of operation the residual shear strain rate is 1 μstrain/yr. Preliminary analysis of strain steps observed at San Juan Bautista during the Morgan Hill earthquake of April 24, 1984, show good agreement with calculations from seismically determined source parameters for this event.

INTRODUCTION

Development and use of shallow, short baseline strain meters have produced general uneasiness on their usefulness in prediction studies except in the study of short-term phenomena. Instrument problems were solved or well understood, but it is now clear that deformation of the near surface due to a wide variety of nontectonic causes severely limits this category of measurement [*Wyatt et al.* 1984; *Linde et al.*, 1982]. Experimentation on the more expensive downhole installations [*Johnston et al.* 1982] clearly indicates that these noise phenomena decrease by as much as 30 dB in the first 200 m, making highly stable strain data available to in-hole instrumentation at this depth.

The most extensively tested continuous borehole strain monitor is the Sacks-Evertson volume strainmeter which has been in use for over 10 years [*Sacks et al.* 1971]. Modeling studies of earthquake-related stress fields indicate that in most cases, knowledge of volume strain is sufficient to determine changes in stress in the earth which could produce precursor signals if these generally exist. Geodetic strain measurements, however, clearly indicate that a large proportion of the significant strain accumulation in California is in simple shear [*Prescott et al.*, 1979]. Thus borehole instruments located at 200–300 m capable of resolving all strain components in the horizontal plane are a valuable means of obtaining localized strain accumulation rates not easily obtainable by other means.

The present installations utilise such a vector instrument, the borehole strain monitor (BVSM), which has previously been used in strain monitoring of underground pillars in hard rock mining applications [*Gladwin*, 1974, 1977, 1982]. The instrument has a useful sensitivity of about 0.3 nstrain and stability measured in these installations of approximately 10 nε/yr (where nε is nanostrain). Dynamic range is approximately 140 dB and linearity better than 0.004% [*Gladwin and Wolfe*, 1975]. The instrument is most useful in simple shear environments where volume strain is minimal, where diagnostic shear strain data are required soon after installation of an instrument, or, as is commonly the case, where large volumetric noise sources such as migration of water tables dominate the strain field.

Two other tensor strain meters have been reported recently. The first [*Sakata*, 1981; *Sakata et al.*, 1982] incorporates three separate sensing volumes in a single instrument package. The annular-shaped sensing volume of the Sacks-Evertson instrument is effectively divided into three regions oriented at 120°. The second [*Chi*, 1982] is based (as is the present device) on capacitance micrometry, also but details of performance have not become broadly available. Both instruments have demonstrated the advantage of shear strain monitoring.

Four types of observations can be achieved with the present instrument: (1) continuous low-frequency borehole tensor strain data for real-time regional deformation monitoring, (2) measurement of elastic and plastic strain offsets generated by nearby earthquakes and the stress redistributions which result, (3) estimates of the absolute state of shear strain when the instrument is implanted in visco-elastic rock immediately after drilling, and (4) observation of dynamic strains associated with the earthquake rupture process.

The present paper reports initial results for the first two types of observations. For the first type of observation the instrument provides accurate continuous deformation monitoring on three axes in a plane perpendicular to the borehole axis. These data may be inverted with due allowance for the perturbation of the remote strain field by the inclusion itself to produce real-time estimates of the hydrostatic and shear field components in the vicinity of the hole.

In the second type of observation the instrument provides direct measurement of the strain step induced at the site by the earthquake rupture. This is related to the seismic moment, and so an array of appropriately located instruments could provide a direct measure of the moment for comparison with

seismically determined moments. One of the instrument sites discussed below was located approximately 60 km from the Morgan Hill (1984) earthquake and provides an example of this type of strain inversion.

The procedure used for the third type of observation, here called postrelief recovery, is useful in estimation of the direction of the in situ maximum shear strain axis and a lower limit on its amplitude. It is related to the common overcoring methods used to determine strain fields in mining applications [Leeman and Hayes, 1966] and more recently in geophysical monitoring [Sbar et al., 1984]. These procedures involve the implantation of a set of deformation gauges into a borehole in a stressed region, followed by total stress relief of the region immediately surrounding the gauges by overcoring. Resulting deformations can be inverted to obtain a measure of the original (ambient) strain and stress state. The procedures are only practicable when close access to the region of interest is available. We here suggest that when this postrelief recovery is monitored by three-component strain instrumentation, the measurements can be used to estimate the minimum in situ shear strain state in crustal rock near active faults or in any material which exhibits viscoelastic behavior without the accessibility limitations of normal overcoring procedures. An instrument with modulus approximately that of the original rock is implanted in a borehole immediately after the borehole drilling process is complete. At this stage the radial stress at the hole boundary is fully relieved, but within the rock mass the strains have not yet been relieved by creep. With time, this strain gradient propagates the ambient strain field back toward the free hole boundary, until a proportion of the original strain field is reconstituted in the rock and instrument implant. The recovery process is exponential and sufficiently slow that the resulting deformations of the instrument can be inverted to yield a lower limit estimate of the state of shear strain prior to drilling. The hydrostatic component of the original strain field cannot be estimated because the creep process is superimposed on both the grout curing process and the thermal recovery following installation. These latter processes are also exponential in form but produce only isotropic deformations in the instrument. Any nonisotropic observed deformation can then be identified with the shear component of the undisturbed shear strain field. An estimate of the static shear at San Juan Bautista site obtained by this technique is the subject of a separate paper. When a borehole has been left open for several months and has therefore largely achieved equilibrium (as was the case for the Pinon Flat installation discussed below), this viscoelastic shear recovery process cannot be observed.

The fourth type of observation, measurement of dynamic strains associated with the passage of seismic waves through the borehole strain instrument sites, has been reported for dilatometers [Johnston et al., 1987] but has not yet been performed with the Tensor strain meters. The installations discussed here are not capable of simultaneous measurement on all components. Instruments for installation in 1986 are setup for simultaneous operation of the sensors. Frequency response of the detection systems is from DC to about 10 Hz.

TECHNICAL DISCUSSION

A detailed description of the instrument has been presented elsewhere [Gladwin, 1984]. In its normal configuration the instrument consists of seven independent components, three of which measure strain in a plane perpendicular to the axis of the instrument. A further two components measure tilt from the axis of the instrument, one component measures the orientation of the instrument in the hole (either by magnetic or gyrocompass), and the final component is a nondeforming reference cell which permits evaluation of the overall performance of the electronics common to all cells and compensation for any time dependent environmentally induced drifts. This component has demonstrated that the instrument stability is better than 10 nε/yr (Figure 2). In the present installations, funding constraints limited the instruments to simple plane strain, so that the two tilt components were not included. The outer diameter of the unit is 125 mm, and it is cemented into 175-mm diameter holes at a target depth in the range 150–200 m. Strain is measured by monitoring the deformation of the instrument diameter to 30 pm in three directions 60° apart. Thermal and other compensations are designed into the geometric configuration of the gauge surfaces. Stability of the instrument at the 1- to 5-year time scale has been achieved by careful machining and fabrication procedures, by controlled destressing of all critical components, and by the use of very high stability (passive ratiometric) electronic techniques in the critical measurement sections. Three components of strain are monitored continuously on the assumption that the strain ellipse is constant over the length of the instrument. The hole is filled with expanding grout for some meters above and below the instrument to produce a near homogeneous inclusion. The device is normally designed to be "moderately hard" with an effective modulus about 0.6–0.8 of that of the host environment. In the present instance, reliable in situ modulii were not attainable at the time of instrument fabrication so that an average modulus value of 20 GPa was chosen. Preferred installation of a vector instrument requires core sampling of representative volumes to determine any anisotropy, to allow determination of in situ modulii necessary for proper inversion of strain data, and to ensure that the instrument site is not contaminated by any local structural geologic features.

Reduction of strains to principal axes is well documented elsewhere [e.g., Jaeger and Cook, 1976; Muskhelishvili, 1953; Savin, 1961]. For a plane stress field the principal strains, ε_1 and ε_2, can be combined to give areal strain (planar hydrostatic strain for the assumption of plane stress conditions) $v = (\varepsilon_1 + \varepsilon_2)/2$ and maximum shear strain $S = (\varepsilon_1 - \varepsilon_2)/2$, where ε_1 is along the axis of maximum compression and $S > 0$. The assumption of plane stress has been made because proximity to the free surface maintains constant stress levels in the vertical direction and because in the region of the instrumented sites, the horizontal stresses are approximately 2–3 times the mean vertical stress at the working depths [Zoback et al., 1980]. Note that for plane stress conditions, the dilation strain Δ is

$$\Delta = \left\{ 2v\frac{(1 - 2v)}{(1 - v)} \right\} \approx 4/3v \approx 2/3(\varepsilon_1 + \varepsilon_2)$$

The general relation for the extensional strain at an angle θ clockwise to this ε_1 axis is [Jaeger and Cook, 1976]

$$\varepsilon(\theta) = v - S^* \cos(2\theta) \qquad (1)$$

For an instrument inclusion subjected to this applied strain

the observed strain $E(\theta)$ is [*Gladwin and Hart*, 1985]

$$E(\theta) = c^*v - d^*S^* \cos (2\theta) \qquad (2)$$

The constants c and d are (planar) hydrostatic and shear response factors generated by the modulus contrast from the surrounding rock. For undisturbed rock, $c = d = 1$, but for normal imperfectly matched inclusions the values of c and d may be determined from knowledge of the elastic constants of the rock, the grout, and the instrument and of the radii of the instrument and the borehole. Values of c in typical strain meter installations range from 1.0 to 2.0 and for d from 2.0 to 4.0. These typical value ranges for the dimensionless constants c and d effectively allow for the fact that an inclusion is more deformable than the undisturbed rock mass and that it is relatively more deformable in shear than in hydrostatic compression. The values of c and d may also be determined from calibration using solid earth tide estimates, but in this presentation all instrument calibrations used have been determined from a priori estimates of instrument and rock parameters. Allowance is made for the effects of the two concentric rings of stainless steel and grout which comprise the inclusion.

Details of this analysis have been presented elsewhere [*Gladwin and Hart*, 1985]. Deformations observed within the instrument for a stress concentration around the borehole are determined by the modulus of the instrument, the expansive grout and the rock, and the thickness of the grout. For three gauges oriented at 60° from each other, extensions u_1, u_2, u_3 can be inverted to provide estimates of the areal (planar hydrostatic) strain v, the maximum shear strain S, and the orientation of the axis of maximum compression ϕ, relative to a reference gauge:

$$v = \frac{(u_1 + u_2 + u_3)}{(3^*c^*r)} \qquad (3)$$

$$\tan 2\phi = \frac{\{3^{1/2}(u_3 - u_2)\}}{\{(u_1 - u_2) + (u_1 - u_3)\}} \qquad (4)$$

$$S = \frac{\{2[(u_1 - u_2)^2 + (u_2 - u_3)^2 + (u_3 - u_1)^2]\}^{1/2}}{(3^*d^*r)} \qquad (5)$$

In this formulation, ϕ is the angle, defined clockwise, from the axis of maximum compression to gauge 3 and r is the instrument inner radius. Note that the angle of the principal stress axes is preserved through the concentric ring structure but the amplitudes observed in a particular gauge direction are modified significantly from that implied in the same direction in undisturbed rock (equation (1)). The formulation in terms of a maximum shear and its orientation in space is chosen since these two quantities are usually of immediate interest in relating observed strain fields to known tectonic features. The choice has implications in the nonlinear algebraic form of the equations (4) and (5) which need careful numeric handling.

For the results described in this paper, the response factors c and d were determined for each instrument site from the analysis of *Gladwin and Hart* [1985] using reasonable estimates of rock and grout modulus. For the Pinon Flat site, $c = 1.9$, $d = 3.5$, and for the San Juan site, $c = 1.3$, $d = 2.5$. The lower values for the San Juan Bautista site reflect the lower rock modulii for this site. An alternative and more complete procedure for the determination of these factors has been described recently [*Gladwin et al.*, 1985]. This procedure uses theoretical (ocean load corrected) tides and observed instru-
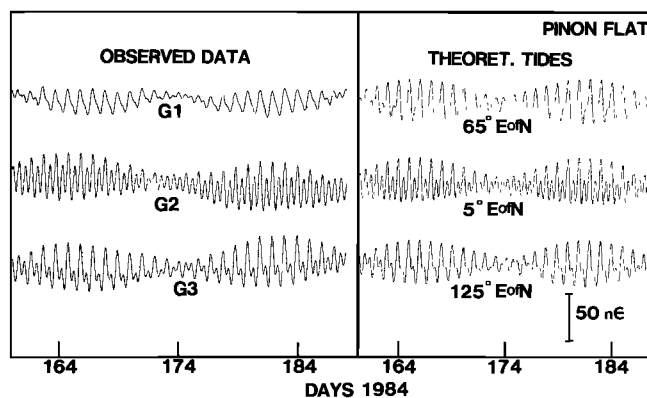

Fig. 1. Comparison of raw 18 min sampled data from the three gauges of the Pinon Flat instrument (simple exponential trend removed) with theoretical calculations of the solid earth tide at the corresponding azimuths (from programs supplied by D. Agnew). The theoretical tides have not been corrected for the effect of ocean loading or topography.

ment tidal deformations to provide an empirical estimate of the hydrostatic and shear response factors for the instruments at each site. Tidal calibration procedures to allow for geologic and topographic inhomogeneities in the surrounding rock and for imperfect bonding of particular component gauges may be possible but have not yet been implemented.

RESULTS

The first site instrumented was at the Pinon Flat Observatory of the University of California, San Diego (33°36'32"N, 116°27'18"W). Installation in a borehole drilled 6 months previously to a depth of 151 m in competent granite was completed September 16, 1983. The axis of gauge 3 was at 125° east of north, with gauge 2 at 60° clockwise, and gauge 1 a further 60° clockwise. The instrument hole was grouted to the surface to minimize thermoelastic contamination by circulation of groundwater. Installation procedures were essentially the same as developed by *Sacks et al.* [1971] at the Department of Terrestrial Magnetism of the Carnegie Institution of Washington for the volume strain meters, in particular in the choice of expansive grout to provide prestress on the instrument.

An example of observed tidal signals at this site is shown in Figure 1. The anomalous low amplitude of gauge 1 is consistent with a correspondingly low tidal amplitude observed on data from the E-W laser strain meter at the same site (F. Wyatt, private communication, 1986). No allowance for this variation has been made in the current data analysis, although a useful procedure is available [*Tullis*, 1981].

Figure 2 shows the performance of the three components since installation. The upper three plots show the actual instrument deformations in nanometers. Combination of these component deformations into planar hydrostatic v and maximum shear S strain is shown in the two lower plots in Figure 2. These curves show the total accumulated strain from initial installation. The dominant areal strain signal is the exponential curing of the expansive grout with a time constant of order 6 months.

The disturbance of the strain measurements evident for a period during December 1984 was caused by additional uneven heat input to the surrounding rock during testing of
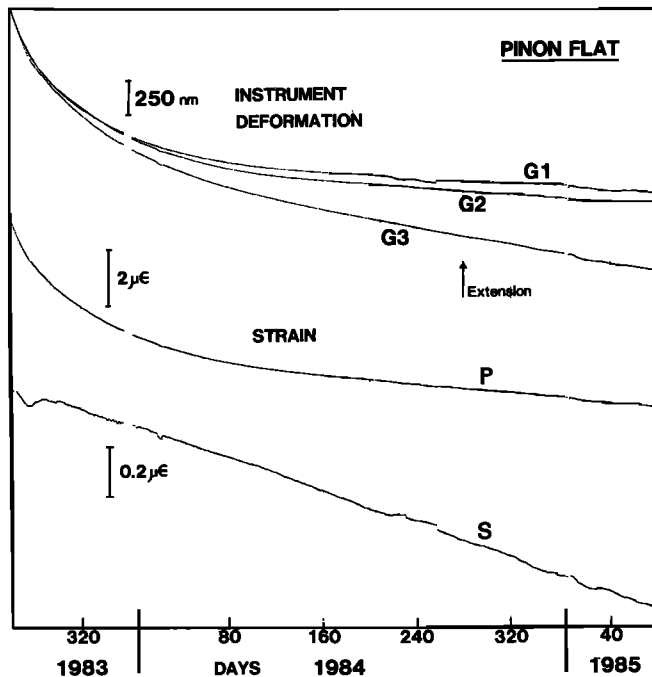
Fig. 2. Performance of the instrument at Pinon Flat since installation (September 15, 1983, day 258). The top three traces labeled G1, G2, and G3 show the deformation of the three strain meter components. Below these are plotted the calculated far-field planar hydrostatic strain P and maximum shear strain S. Note that vertical scales for the two strain fields are different.

the capability of the system for high sample rate high gain recording on one component of this instrument. The disturbance on gauge 1 during August 1984 has not yet been explained.

The most significant feature of this data is the emergence of an apparently constant accumulation of maximum shear (approximately 0.6 μstrain tensor shear per year) which was established within 2 months of installation. The azimuth of the maximum compression axis of this shear, as discussed later, is oriented at N50° ± 5°W. In a stress relieved borehole, only far-field shear accumulations would be observed during the hydrostatic curing stage. The present data set shows a remarkably constant shear strain rate, independent of the hydrostatic recovery process. The imposed shear strain accumulation rate is a factor of 10 higher than geodetic average estimates for the region quoted as 0.05 ± 0.03 $\mu\varepsilon$ (engineering shear) per year by King and Savage [1983]. Some variation in the strain due to distance from the San Andreas and San Jacinto fault lines has been documented by King and Savage [1983], who show variation between 0.05 and 0.15 $\mu\varepsilon$/y over their shear strain rate profile. Local topographic effects [Harrison, 1976] are also to be expected but not at this level. Berger and Beaumont [1976] reported variation of 25% in the M_2 and O_1 components of the tides at Pinon Flat observatory when topological and geological corrections were applied, and this is a reasonable upper limit of expectation for the secular strain variation.

The most direct explanation of the discrepancy is to assume that the mechanical reference for gauge 3 was disturbed during installation so that it has an abnormal mechanical gain. These reference gauges are set to better than 0.5% during fabrication, and it is unlikely that the error required (approximately 50%) to reduce the present shear to the

average levels obtained from the long baseline geodetic measurements over the area could occur without producing also evidence of poor mechanical stability. Furthermore, earth tide amplitudes for this component gauge are not abnormally high. We believe that this explanation is unlikely. We have also examined the effects on observations caused by the deviation of the hole from the vertical (4.5° in a direction S35°W in this case) and find that the measured shear is not produced by this deviation.

The stability of the measurement system itself can be evaluated from the performance of the fourth (noncoupled) reference gauge included in the borehole package. In the interval from the beginning of 1984 to the beginning of 1985, the total indicated drift on this element is less than 1.4 nm which represents approximately 10 $n\varepsilon$. From the internal consistency of the data and from the instrumental checks included in the system we would therefore argue that the data are real at the instrument.

The most likely cause of this constant trend is long-term viscoelastic response of the rock due to the presence of the borehole [Berry, 1967; Barla and Wane, 1968]. It is evident from both installations that long-term strain rates approach a constant nonzero value when grout curing effects have ended. The inclusion modulus is less than that of the surrounding medium, and a static stress gradient exists between the hole and its environment. If the response of the rock is assumed to be that of a Burgess solid in a stressed environment, the constant drift rate would be a measure of the Maxwell element of the creep coefficient of the medium.

Whatever the cause of this very linear trend in the shear data, it is clear that fluctuations of shear strain rate larger than 100 $n\varepsilon$/yr would readily detected. In terms of the immediate objectives of the present experiments, fluctuations in strain rate exceeding this low measured noise threshold are of significance. Direct comparison with laser interferometer measurements at Pinon Flat are in progress but will probably be inconclusive in the short term due to difficulties in obtaining an equally stable secular shear strain rate from the interferometer (only one component of the interferometer is presently capable of equivalent stability for secular studies). It is probable, however, that the laser data are closer to geodetic estimates than to our measured data. The laser data are, of course, not subject to the hole effects discussed above.

The second installation was at San Juan Bautista at a distance of 1.2 km from the San Andreas fault and in close proximity to several U. S. Geological Survey (USGS) strain monitoring sites (36°50'1"N, 121°32'34"W). This region is of tectonic interest because of strong fault displacement gradients [Savage et al., 1979] and continuing high seismicity. The installation was completed within 6 days of the completion of the drilling and at a depth of 148 m. For this site, gauge 3 was oriented 205° east of north, with gauges 2 and 1 each a further 60° clockwise. The site was in a poorly sorted sandstone with high clay content. Figure 3 shows the performance of this site over the first 18 months of operation. The upper traces are again deformation, and the lower two are the computed strain. All three components show tidal signals with approximately correct phase angles indicating proper coupling on each component. Analysis of the data at this site is made difficult by the presence of an open borehole 140 m deep approximately 8 m to the south of the tensor instrument. This very close open hole intended for another instrument type certainly couples atmospheric effects directly into the instrument and may also

permit migration of the water tables. A close examination of the data indicates that two exponential processes are involved at this site, the first with a time constant of 10 days, the second with a time constant of order 6 months. The second process is identified with grout curing and areal strain v shows an expected exponential decay of approximately 6 $\mu\varepsilon$ during this time period. This is consistent with the Pinon Flat result for similar hole geometry. The short time constant exponential process which is clearly not caused by grout cure can be explained as a viscoelastic recovery of the stress relieved during drilling. It it detectable only because the implant was completed soon after the drilling was completed. The plot of shear strain S contrasts strongly with that observed at the Pinon Flat Observatory site (see Figure 2). The strain recovery is indicated on both P and S components and is superimposed on the grout cure compression. It is evident in Figure 6 that the measured angle of maximum shear direction continues to be that of the original static field direction inferred during the initial recovery phase.

Savage et al. [1979] have documented the shear strain rate in the block to the southwest of the San Andreas fault at less than 0.10 $\mu\varepsilon$/yr and an upper limit of 0.62 $\mu\varepsilon$ (engineering) per year for the whole region. The measured shear shown in Figure 3 is, clearly, not imposed from this secular strain rate. It is a measure of the preexisting shear strain state in the vicinity of the borehole not relieved during the short time between drilling of the hole and implant of the instrument. The data indicate an axis of maximum compression at N10° ± 3°W. This agrees closely with the value of N4° ± 3°W obtained by both hydrofracture techniques [Zoback et al., 1980] and geodetic surveys [Prescott et al., 1979].

Since the hole curing process is not yet complete, a

Fig. 4. Rate of change of maximum shear S plotted for each site. This is calculated by averaging the data from each gauge over a 5-day period, then determining the change in deformation from one 5-day period to the next. These changes are then combined using the equations described earlier to obtain S and P.

measurement of the secular shear accumulation rate at this site is not yet possible. The measured shear strain rate after two years at this site has decreased to approximately 1.0 μstrain/yr (somewhat larger than that observed at the Pinon Flat site for the viscoelastic hole response).

An estimate of the rate of change of S and P for both sites is obtained from readings differenced over a short time interval. Figures 4 and 5 illustrates the rates calculated from 5-day differences, for the 1984 data set. The constant rate of accumulation of maximum shear (0.6 μstrain/yr) revealed for Pinon
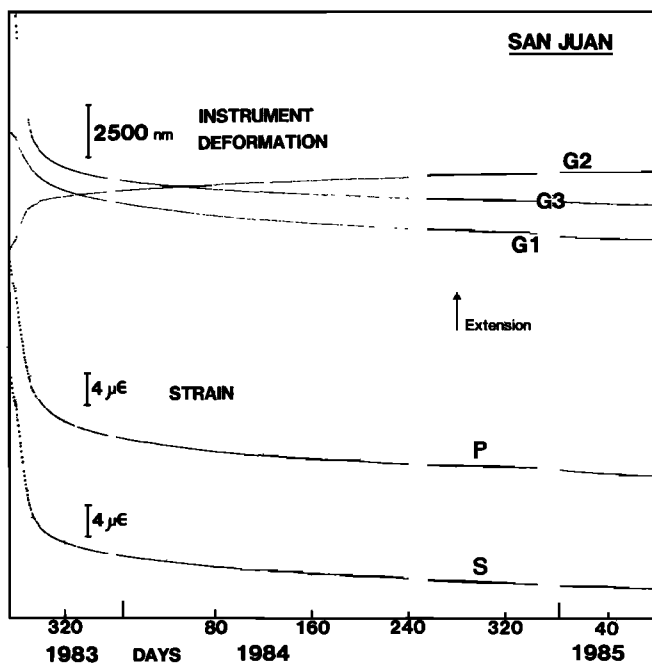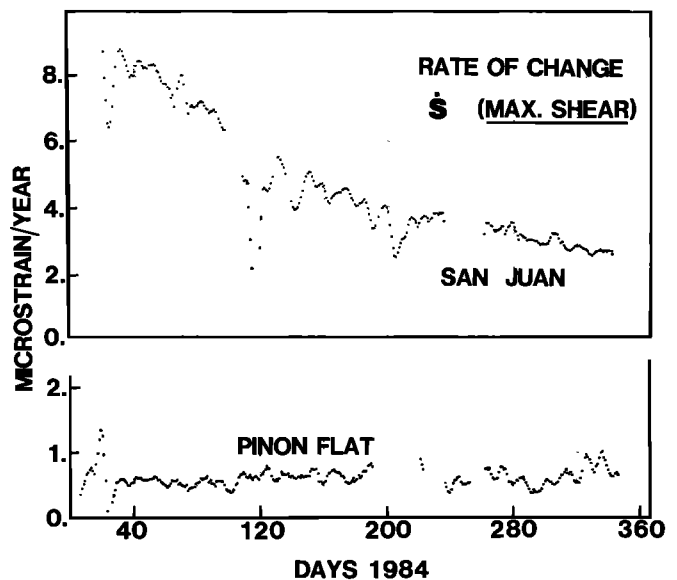

Fig. 3. Data from the San Juan instrument since installation (September 28, 1983, day 271). Top three traces labeled G1, G2, and G3 show the three component deformations. Resulting plots for P and S are also shown. At this site, hole drilling was completed 6 days prior to installation. The stress recovery following the drilling process is indicated by the large exponential decay of S in the early part of the figure.
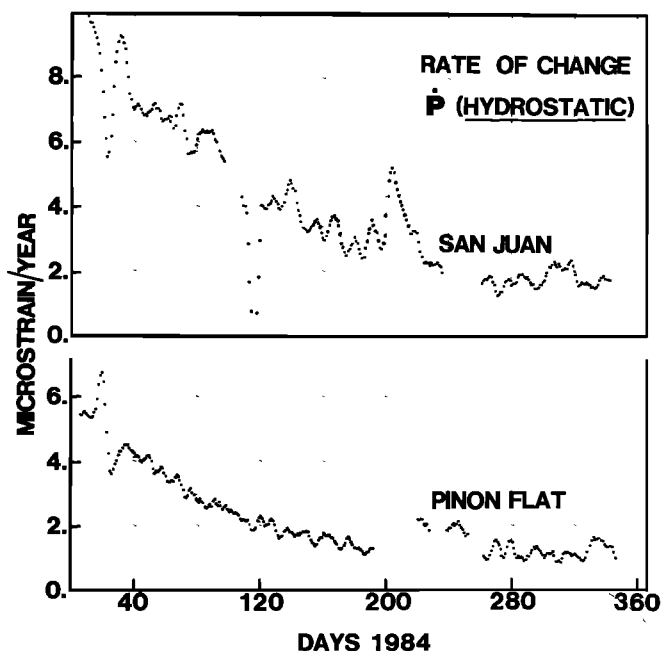

Fig. 5. Rate of change of hydrostatic strain P for each site. This is calculated as described for Figure 4. The decrease in rate of compression is caused by curing of the grout.
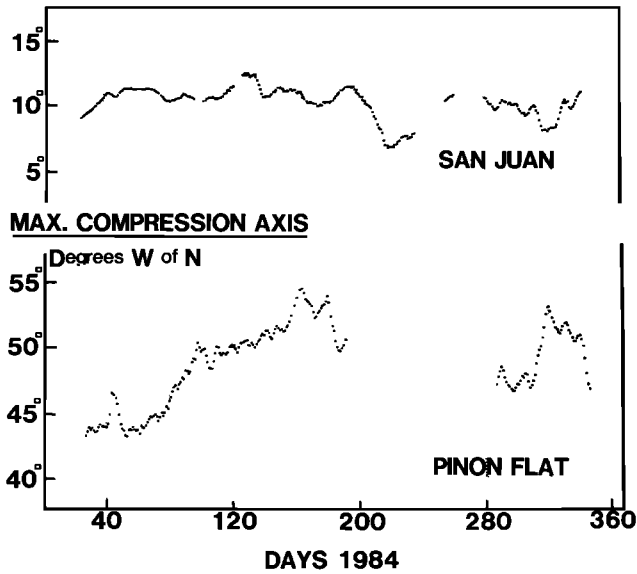
Fig. 6. Angle of maximum compression plotted for each site. This is calculated by the procedure described for Figure 4, except that in this case, 25-day differences were used.

Flat in Figure 2 is clearly evident in Figure 4. This contrasts strongly with the data for the San Juan site shown in Figure 4. The hydrostatic response curves in Figure 5 for the two sites are equivalent, being controlled by grout curing and in situ modulus. Some of the structure evident in these data is an artifact of the difference window selected, in this case 5 days.

Figure 6 shows the principal strain axis (maximum compression) for the two sites, calculated from 25-day differences of gauge readings. Each 25-day interval produces an independent measure of the angle of the maximum principal axis with-

out undue dependence on the chosen starting point. Fluctuations apart from those relating directly to the chosen window length give some indication of the stability of the estimate. The relatively low rate of shear change leads to the angle being less well defined for the Pinon Flat data, the angle being determined (equation (3)) from ratios of smaller differences of gauge readings. This axis of maximum compression appears to have shifted since the start of 1984 from N44° ± 5°W to 50°W. This axis differs significantly from the averaged result for the region (N2° ± 5°) obtained by geodetic means [Prescott et al., 1979]. However, the shears involved are small, and so the orientations are poorly determined in either system.

An example of the response of this instrument to an earthquake is shown in Figure 7 for the Morgan Hill earthquake on April 24, 1984 ($M = 6.2$ at epicentral distance of 60 km). The coseismic offsets are seen on all three components, with indications of continued or triggered postseismic slip on two components (2.25 nm on gauge 1 and 13.25 nm on gauge 3). The coseismic offsets can be modeled using fault parameters derived from seismic observations [Gladwin and Johnston, 1984]. One simple model consistent with the seismic data uses slip of 42 cm between 5 and 10 km over a 30-km rupture length striking in the N33°W direction. This model, which also models well the borehole dilatometer observations at Searle Road, a site 5 km to the northwest of the present installation [Johnston et al., 1985], predicts coseismic offsets at the instrument site in reasonable agreement with observations. The component values shown in Figure 7 have not been corrected for the effects of the hole response. The observations indicate a hole corrected areal strain of 103 ne and maximum shear of 68 ne at an angle N55°W for this site. These should be compared with the model values of 105 ne areal strain and 152 ne maximum shear at N63°W. Although the amplitude of the hydrostatic component and the angle of the maximum shear axis are moderately well determined, the amplitude of the
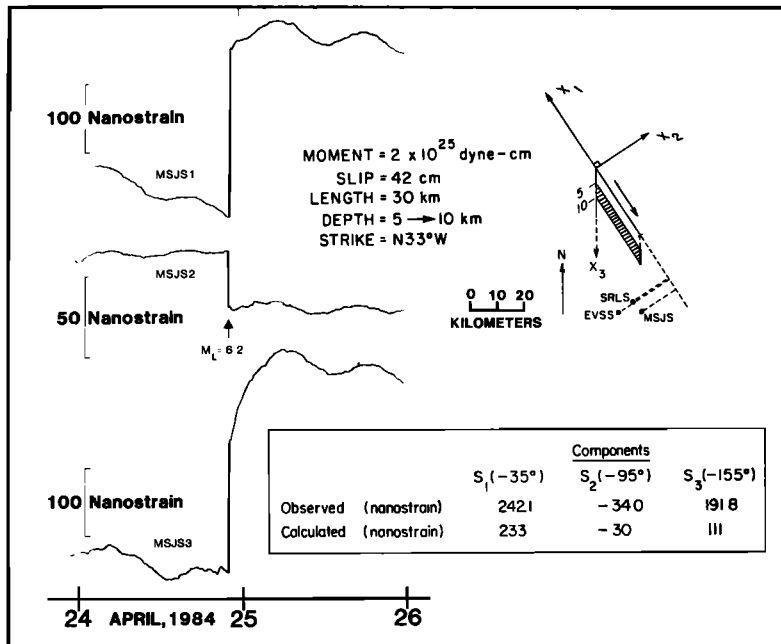

Fig. 7. Composite data for the Morgan Hill event. The time series for each component spanning the event occupies the left side of the figure and reveals an elastic event followed by a significant plastic deformation over the next several hours. The site location in relation to the seismically determined fault plane solution is shown in the upper right, and a comparison of computed and observed strains (not hole corrected) at the site is shown in the lower right.

maximum shear strain has been underestimated. Given that the region between the Morgan Hill epicenter and the instrument site is highly complex, being intersected by more than one active fault trace, we do not expect perfect agre ment with the source model, or that one isolated instrument can adequately map the source region. It is probably significant that only the shear strain amplitude is significantly in error, since it has been demonstrated [*Johnston*, 1983] that shear strain concentration occurs in region of low modulus along fault zones. This has the effect of decreasing the shear component but not the hydrostatic component of a strain field observed from the remote side of a fault zone by as much as 30% at each fault crossing for a fault modulus of 50% of the surrounding rock. The postseismic effect indicates an additional hydrostatic component of 32 nε and an additional maximum shear of 26 nε at an angle N25°W.

The results here presented have been obtained using a priori instrument clibrations only and are expected to improve when tidal calibration procedures allow independent in situ calibration of the response of each gauge. These tidal calibration procedures will also permit evaluation of the performance of each gauge.

CONCLUSION

The data presented for Pinon Flat indicate the stability to be expected of this type of instrumentation in a quiet tectonic environment and suggest that changes of the rate of shear strain accumulation larger than 100 nε/yr can readily be detected. The data from the San Juan site illustrate the use of tensor borehole instrumentation for inversion of coseismic and postseismic strain fields and show good concordance with seismic parameters. In situ calibration procedures are essential to allow interpretation of the data at the achieved level of stability of the instrument.

REFERENCES

Barla, G., and M. T. Wane, Analysis of the borehole stress-relief method in rocks with rheological properties, *Int. J. Rock Mech. Min. Sci., 5,* 187–193, 1968.

Berger, J., and C. Beaumont, An analysis of tidal strain observations from the United States of America, *Bull. Seismol. Soc. Am., 66,* 1821–1846, 1976.

Berry, D. S., Deformation of a circular hole driven through a stressed viscoelastic material, *Int. J. Rock Mech. Min. Sci., 4,* 181–187, 1967.

Chi, S.-L., Preliminary results of a capacitance-type borehole earth strain meter, *Acta Seismol. Sin., 4,* 98–103, 1982.

Gladwin, M. T., Ultrasonic stress monitoring in active sites: Observation of the time dependence of stress relief mechanisms in mining pillars, *Eos Trans. AGU, 55,* 1192, 1974.

Gladwin, M. T., Simultaneous monitoring of stress and strain in massive rock, *Pure Appl. Geophys., 115,* 267–274, 1977.

Gladwin, M. T., Ultrasonic stress monitoring in underground mining, *Int. J. Rock, Mech. Min. Sci. Geomech. Abstr., 19,* 221–228, 1982.

Gladwin, M. T., High precision multi component borehole deformation monitoring, *Rev. Sci. Instrum., 55,* 2011–2016, 1984.

Gladwin, M. T., and R. Hart, Design parameters for borehole strain instrumentation, *Pure Appl. Geophys., 123,* 59–88, 1985.

Gladwin, M. T., and M. J. S. Johnston, Strain episodes on the San Andreas fault following the April 24 Morgan Hill, California earthquake, *Eos Trans. AGU, 65,* 852, 1984.

Gladwin, M. T., and J. Wolfe, Linearity of capacitance displacement transducers, *J. Sci. Instrum., 46,* 1099–1100, 1975.

Gladwin, M. T., R. Hart, and R. L. Gwyther, Tidal calibration of borehole tensor strain meters, *Eos Trans. AGU, 66,* 1057, 1985.

Harrison, J. C., Cavity and topographic effects in tilt and strain measurement, *J. Geophys. Res., 85,* 319–328, 1976.

Jaeger, J. C., and N. G. W. Cook, *Fundamentals of Rock Mechanics,* 2nd ed., section 10.4, Chapman and Hall, London, 1976.

Johnston, M. J. S., The need for interactive earthquake instability models, paper presented at IUGG XVIII General Assembly, Int. Assoc. of Seismol. and Phys. of the Earth's Inter., Hamburg, Aug. 15–27, 1983.

Johnston, M. J. S., A. T. Linde, I. S. Sacks, and D. Myren, Borehole dilatometer strain array—Preliminary results from Mojave Desert, *Eos Trans. AGU, 63,* 430, 1982.

Johnston, M. J. S., M. T. Gladwin, and A. T. Linde, Preseismic failure and moderate earthquakes paper presented at 23rd General Assembly, Int. Assoc. of Seismol. and Phys. of the Earth's Inter., Tokyo, Aug. 19–30, 1985.

Johnston, M. J. S., A. T. Linde, M. T. Gladwin, and R. D. Borcherdt, Fault failure with moderate earthquakes, *Tectonophysics,* in press, 1987.

King, N. E., and J. C. Savage, Strain-rate profile across the Elsinore, San Jacinto, and San Andreas faults near Palm Springs, California, 1973–1981, *Geophys. Res. Lett., 10,* 55–57, 1983.

Leeman, E. R., and D. J. A. Hayes, Technique for determining the complete state of stress in rock using a single borehole, paper presented at the 1st Congress, Int. Soc. of Rock Mech., Lisbon, 1966.

Linde, A. T., I. S. Sacks, R. Stefansen, F. Wyatt, and M. S. J. Johnston, Noise in near surface measurements of earth strain, *Eos Trans. AGU, 63,* 1118, 1982.

Muskhelishvili, N. I., *Some Basic Problems of the Mathematical Theory of Elasticity,* translated by J. R. M. Radok, P. Noordhoff, Groningen, Holland, 1953.

Prescott, W. H., J. C. Savage, and W. T. Kinoshita, Strain accumulation rates in the western United States between 1970 and 1978, *J. Geophys. Res., 84,* 5423–5435, 1979.

Sacks, I. S., S. Suyehiro, D. W. Evertson, and Y. Yamagishi, Sacks-Evertson strainmeter, its installation in Japan and some preliminary results concerning strain steps, *Pap. Meteorol. Geophys., 22,* 195–208, 1971.

Sakata, S., On the concepts of some newly invented borehole three component strain meters, report, Natl. Res. Cent. for Disaster Prevent., Tokyo, 1981.

Sakata, S., S. Shimada, and S. Noguchi, Continuous crustal strain observation in the Kanto District, A tripple junction area, by new type three component borehole strainmeters, paper presented at General Meeting, Int Assoc. of Geod., Tokyo, 1982.

Savage, J. C., W. H. Prescott, M. Lisowski, and N. E. King, Geodolite measurements of deformation near Hollister, California, 1971–1978, *J. Geophys. Res., 84,* 7599–7615, 1979.

Savage, J. C., W. H. Prescott, M. Lisowski, and N. E. King, Strain accumulation in southern California, 1973–1980, *J. Geophys. Res., 86,* 6991–7001, 1981.

Savin, G. N., *Stress Concentration Around Holes,* Translated by W. Johnson, chapter 5, Pergamon, New York, 1961.

Sbar, M. L., R. M. Richardson, and C. Flaccus, Strain relaxation measurements on the San Andreas fault in southern California, *J. Geophys. Res., 89,* 9323–9332, 1984.

Tullis, T. E., Stress measurements via shallow overcoring near the San Andreas fault, in *Mechanical Behavior of Crustal Rocks, Geophys. Monogr. Ser.,* vol. 24, edited by N. L. Carter, M. Friedman, J. M.

Logan, and D. W. Stearns, pp. 199–214, AGU, Washington, D. C., 1981.

Wyatt, F., R. Bilham, J. Bevan, A. G. Sylvester, T. Owen, A. Harvey, C. Macdonald, D. D. Jackson, and D. C. Agnew, Comparing tilt-meters for crustal deformation measurement—preliminary report, *Geophys. Res. Lett., 11*, 963–966, 1984.

Zoback, M. D., H. Tsukahara, and S. Hickman, Stress measurements at depth in the vicinity of the San Andreas fault: Implications for the magnitude of shear stress at depth, *J. Geophys. Res., 85*, 6157–6173, 1980.

M. Francis, M. T. Gladwin, R. L. Gwyther, and R. Hart, Department of Physics, University of Queensland, St. Lucia, 4067 Australia.

M. J. S. Johnston, U. S. Geological Survey, 345 Middlefield Road, MS977, Menlo Park, CA 94025.